Article

Inferred nutrient forcing on the late middle Eocene to early Oligocene (~40–31 Ma) evolution of the coccolithophore *Reticulofenestra* (order Isochrysidales)

Ruigang Ma[1,2] , Marie-Pierre Aubry[2], David Bord[2,3], Xiaobo Jin[1] and Chuanlian Liu[1]

[1]State Key Laboratory of Marine Geology, Tongji University, Shanghai 200092, China
[2]Department of Earth and Planetary Sciences, Rutgers University, New Brunswick, New Jersey 08854, U.S.A
[3]Ellington Geological Services, 1414 Lumpkin Road, Houston, Texas 77043, U.S.A

Non-technical Summary

Coccolithophores are unicellular algae, with the cell surface covered by calcite scales (coccolith). Coccolithophore size has become progressively smaller from the late Paleogene to the present. The first size reduction (FSR) occurred ~32 million years ago in the most successful modern lineage, the order Isochrysidales. To decipher the driving mechanism(s) behind the FSR, we conducted a morphologic analysis on the fossils of coccolithophores that lived during the late middle Eocene to early Oligocene (~40–31 million years ago), using marine sediments from the South Atlantic Ocean. Our data show a strategic divergence between groups of large and small coccolithophores. The group of larger coccolithophores increased in size by ~4 μm before their extinction, while the size range of the group of smaller coccolithophore contracted. In addition, the central opening on the coccolith decreased in all species from the late Eocene to early Oligocene. We infer that the increased nutrient availability during the Eocene/Oligocene climate transition may be responsible for the morphologic evolution. We hypothesize that larger species with larger central openings on their coccoliths were more dependent on mixotrophy, making them better adapted to the nutrient-poor conditions from the middle to late Eocene. On the other hand, smaller species whose central opening dwindled were better adapted to nutrient-rich conditions during the early Oligocene. Our inference supports the idea that the diversity of trophic strategies among phytoplankton is underestimated.

Abstract

The first size reduction (FSR) in the *Reticulofenestra-Gephyrocapsa-Emiliania* (*RGE*) lineage (order Isochrysidales), which occurred in the early Oligocene (~32 Ma), is of great significance for understanding the Lilliput effect that has affected coccolithophore communities from the late Eocene to this day. We conducted a morphologic analysis on the coccoliths of *Reticulofenestra* species that lived during the late middle Eocene to early Oligocene (~40–31 Ma), using marine sediments from the South Atlantic Ocean. Our data show increasing size and decreasing abundance of the large species during the late Eocene, leading to their disappearance at the FSR, and a concurrent decrease in the size variability of the small- to medium-sized coccoliths whose central opening diameter had become very reduced. Although the cosmopolitan late Paleogene through Neogene size decrease in coccolithophores has been linked to the concomitant long-term decline in global $p\mathrm{CO_2}$, we suggest here that the FSR was the result of environmental destabilization caused by the expansion of eutrophic environments following the late Eocene establishment of overturning circulation associated with ice buildup on Antarctica. This study also leads us to propose a hypothetical model that links coccolith morphology of species of the *RGE* lineage and trophic resources in the upper ocean: the small- to medium-sized, r-selected coccolithophores with smaller coccolith central openings live in nutrient-rich waters where they rely mostly on photosynthesis and little on mixotrophy, whereas the larger, K-selected species with larger coccolith central openings live in oligotrophic waters where they are more dependent on mixotrophy.

Introduction

Coccolithophores are calcifying, unicellular, planktonic algae that contribute up to 20% of the organic carbon fixation in the upper ocean (Poulton et al. 2007) and about half of the deep-sea carbonate precipitation (Milliman 1993). Because of their rapid evolution, the products of their calcification, coccoliths and coccospheres, have long been used in Earth sciences, not only to

date sediments (e.g., Martini 1971; Backman et al. 2012) but also to characterize major biotic events since the Late Triassic, when they became common in marine sediments (e.g., Bown et al. 2004; Suchéras-Marx et al. 2019). Following the Cretaceous/Paleogene mass extinction, the coccolithophores underwent bursts of diversification, reaching their highest diversity during the early Eocene climatic optimum (EECO). Subsequently, global cooling and associated oceanic eutrophication fueled the diversification and spreading of opportunistic (r-selected) species, leading to an early Oligocene bottleneck of the entirety of coccolithophore diversity (Bown et al. 2004; Aubry and Bord 2009; Hannisdal et al. 2012; Henderiks et al. 2022). While the major K-selected taxonomic groups became sequentially restricted, species of the genus *Reticulofenestra* increased in abundance, leading to their dominance in the Oligocene coccolithophore communities (Aubry 1992). *Reticulofenestra* appeared during the EECO (Agnini et al. 2006), and except for one species, disappeared in the late Pliocene. It gave rise to *Gephyrocapsa* in the late Miocene, from which *Emiliania* evolved in the Pleistocene (Perch-Nielsen 1985; Gibbs et al. 2005), both of which dominate living communities (e.g., Poulton et al. 2017).

The *Reticulofenestra-Gephyrocapsa-Emiliania* lineage (RGE) is of great interest, because it shows the same Lilliput effect that affected all coccolithophores during the Neogene (Aubry 2007, 2009; Fig.1)—a size decrease along lineages that is not yet fully understood. The *RGE* lineage belongs to the family Noelaerhabdaceae Jerkovic, 1970 (Young and Bown 1997) of the order Isochrysidales Pascher, 1910, and the taxonomically complex *Reticulofenestra* group is often referred to as reticulofenestrids. Although marked by pervasive iterative evolution (Matsuoka and Okada 1990; Young 1990; Bendif et al. 2019), the first selection for small size in the lineage marks the Eocene/Oligocene transition, when species with coccoliths ≥14 μm disappeared (Backman and Hermelin 1986). No species of the *RGE* lineage with comparable size would evolve thereafter. Thus, in light of their Neogene evolution toward a small size, a documentation of this first, distinctive event, which is dubbed here the "first size reduction" (FSR), holds the potential to shed light on size and shape selection forcing mechanisms in *Reticulofenestra* and to confirm or nuance existing interpretations of size change forcing mechanisms among species of the *RGE* lineage through the Neogene and up to the present (Fig. 1).

We present here the results of a morphometric analysis of the *Reticulofenestra* coccoliths preserved in the upper Eocene through lower Oligocene chalks from the South Atlantic Ocean, focusing on three morphologic parameters— coccolith length, central opening/coccolith length ratio, and circularity. The forcing mechanisms that possibly drove changes in these morphologic traits are discussed in the context of the Eocene–Oligocene climatic changes at a million-year temporal resolution. We conclude with a hypothetical ecological model that attempts to relate morphology of the *RGE* coccoliths with the ecological and/or physiological requirements of their species and that may well be applicable to other coccolithophores.

Material and Methods

Material

We analyzed 32 samples taken at intervals of ∼50 cm in cores from a 100-m-thick section of upper Eocene through lower Oligocene chalks from Deep Sea Drilling Project (DSDP) Site 363 in the eastern South Atlantic Ocean (19°39′S, 09°03′E; Bolli et al. 1978; Fig. 2) between Core 5, section 5, 80 cm, and Core 10, section 5, 45 cm (∼114–212 m below seafloor [mbsf]). Coring was discontinuous at this site, but a preliminary analysis showed that the FSR is well represented in the continuously recovered Core 7 (Proto Decima et al. 1978) and that the section yielded consistent information.

Calcareous nannofossils were abundant and well to moderately well preserved in all samples except in the bottom of Core 7 (155 mbsf) and in the upper part of Core 8 (∼165 mbsf), which were omitted from the analysis. *Reticulofenestra* coccoliths were abundant in the chalks sampled for this study, representing ∼60–90% of the assemblages (Supplementary Fig. S1). Their preservation was good, although with minor evidence of overgrowth that we have quantified (Supplementary Plate S1).

Reticulofenestra Coccoliths. *Reticulofenestra* coccoliths are elliptical to circular placoliths. Their structure was first comprehensively described by Stradner in his emendation of the genus (Stradner in Stradner and Edwards 1968), with further information given by Driever (1988), Gallagher (1989), and Young (1989); they are abundantly illustrated in numerous studies (e.g., Perch-Nielsen 1971; Wise 1983). The *Reticulofenestra* placoliths consist of two superposed shields that delineate a tubular central opening similar in shape to the coccolith. The central opening is closed by a thin, porous layer of anastomosed elements, which extend from the elements of the proximal shield. The central opening may also be spanned distally by a coarser structure that exhibits a diversity of configurations. The variable and often transitional structure of the central area has resulted in a complex and sometimes controversial taxonomy of the genus *Reticulofenestra*, with one to four generic names in common use depending on the authors. Species taxonomy is based on the morphology of the coccoliths and the structure of their central area, implying that species concepts in paleontology are based on coccolith morphotypes. Even so, the delineation of paleontological species in *Reticulofenestra* is rendered difficult by overlapping characters and iterative evolution, and size is often used as a primary specific character. Thus, for the purpose of this study, we examine all (paleontological) species collectively except *Dictyococcites*, whose central opening is difficult to delineate accurately for measurement. The species composition is constant throughout the studied interval, although the loss of the large species *Reticulofenestra umbilicus* Martini and Ritzkowski 1968 and *Reticulofenestra hillae* Bukry and Percival 1971 at ∼32 Ma constitutes a prominent event that is part of the FSR. Backman and Hermelin (1986) showed from nearby Site DSDP 523 that the large species *R. umbilicus* originated in the middle Eocene following a progressive size increase between ∼45 and 43 Ma and that a subsequent shrinking of the central opening led to the occurrence of the ecophenotypic species *R. hillae*. The abrupt and synchronous extinction of both species marks the boundary between Biozones NP22/NP23 (Martini 1971) and Biozones CNO2/CNO3 (Agnini et al. 2014). It is one of the most prominent events of the Oligocene timescale, although a comprehensive morphologic study of this event at ∼32 Ma has been lacking. The species with smaller (∼6 μm), subcircular placoliths that dominated Oligocene *Reticulofenestra* communities after the FSR belong to *Reticulofenestra floridana* (Roth and Hay, 1967 in Hay et al. 1967) Theodoridis 1984. For further information on *Reticulofenestra* taxonomy, the reader is referred to Nannotax3 (www.mikrotax.org/
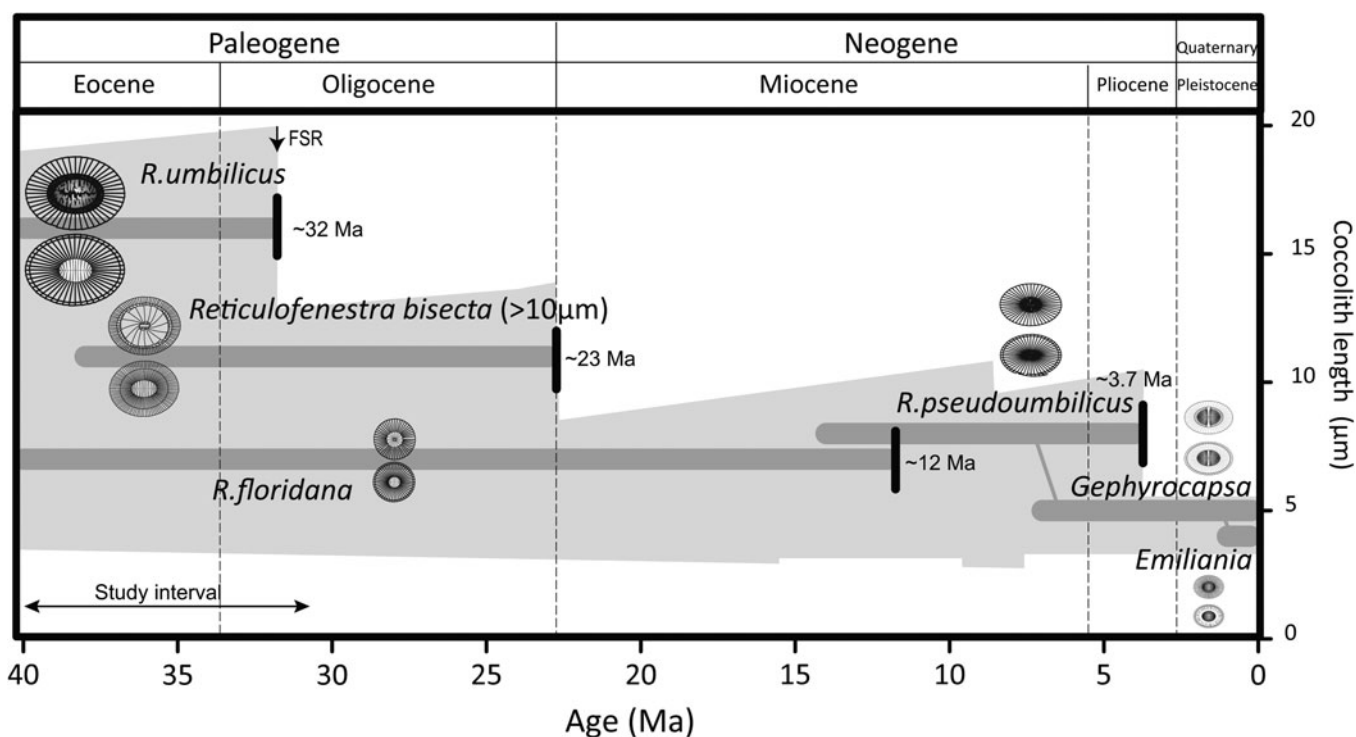
Figure 1. History of size in the *Reticulofenestra-Gephyrocapsa-Emiliania* lineage (modified from Aubry 2007). The gray shaded area shows the variations in size of all the species of the *RGE* lineage through the late Paleogene, Neogene, and Quaternary placed in a numerical temporal framework based on studies by Matsuoka and Okada (1990), Young (1990), Gibbs et al. (2005), Henderiks (2008), Imai et al. (2015), and this study. Coccoliths are shown in distal and proximal view. Major size changes correlative with the extinctions of main taxa (genera or species) are highlighted (thickened lines). Two main events are the first and last reductions in size (FRS and LRS, respectively) at ~32 Ma and 3.7 Ma. The extinction of the small- and medium-size circular placoliths at ~12 Ma is also shown. Note that species *bisecta* is assigned to *Reticulofenestra* by some authors and to *Dictyococcites* by others and that the largest coccoliths (≥10 μm) of this species are also named *D. stavensis* (e.g., Bordiga et al. 2015).

Nannotax3, to which the reader is also referred for all other taxa cited in this work).

Sample Preparation. All samples were prepared from dispersion in water of a small amount of chalk deposited on a cover slip and mounted on a glass slide after evaporation of the water (Corliss et al. 1984). The smear slides were analyzed at a magnification of 1000× using a Zeiss Axioplan 2 polarized light microscope coupled with Zeiss software AxioVision40 v. 4.8.2.
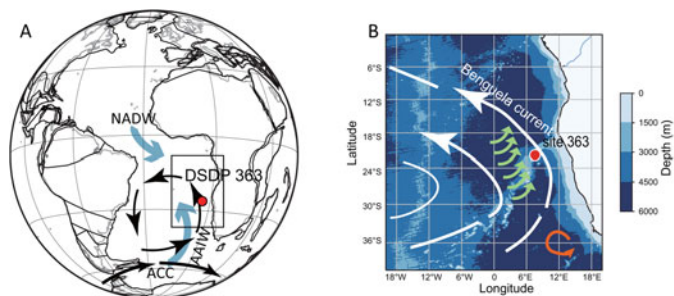

Figure 2. Paleoceanographic reconstruction of the late Eocene South Atlantic Ocean (A) and location of Deep Sea Drilling Project (DSDP) Site 363 (B). Plate tectonic reconstruction map (A) generated from www.odsn.de. The region of the Walvis Ridge is currently under the influence of the Benguela Current (B), which is the eastern portion of the South Atlantic Ocean Gyre (white arrows). A coastal upwelling system (green arrows) developed as a result of this current. ACC, Antarctic Circumpolar Current; AAIW, Antarctic Intermediate Water; NADW, North Atlantic Deep Water.

Morphometric Analysis

Morphometric Measurements. Morphometric measurements were performed by randomly taking photographs under bright-field conditions of 10 to 15 fields of view per smear slide at 1000× magnification. A field of view typically contained 5 to 10 *Reticulofenestra* placoliths. For each sample, 100 specimens were measured. To avoid distortion caused by different orientations of the coccoliths as seen in light microscopy, only specimens horizontally oriented with the microscope stage were measured.

Measurements were conducted manually using the biometric analysis software Fiji v. 1.52 P (Schindelin et al. 2012) by dragging ellipses over the contours of each placolith in order to measure its length and width. The long and short diameters of the central opening were likewise measured. Our procedure has resulted in a database of 6400 measurements for the whole study.

To estimate the uncertainty in our measurements, we selected three specimens from three different smear slides, ranging from the smallest to the largest placoliths, and measured the images of each one 20 times. The error was ~0.14 μm for the largest specimens (mean = 13.3 μm) and ~0.15 μm for the smallest specimens (mean = 4.5 μm). In addition, we randomly took five samples and measured 180 specimens in each. The results show minor differences (≤0.2 μm) in mean values between the two sampling sizes. The accuracy of the measuring method thus fulfills the needs of this study (Supplementary Fig. S2).

We undertook a morphometric analysis with the double objective of quantifying the morphologic features of the placoliths at
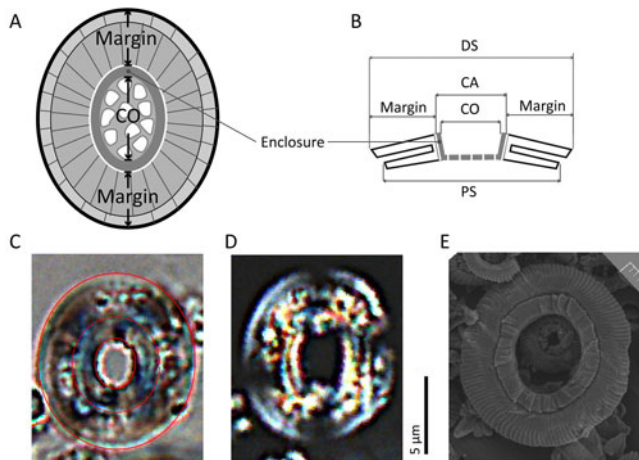
Figure 3. Morphology of a *Reticulofenestra* coccolith (placolith) and measured parameters. A, Interpretative drawing of the proximal (internal) face showing the margin composed of two superposed shields and the central area, which is outlined by the enclosure (or tube cycle) and spanned by a proximal reticulum. B, Axial longitudinal section. C, Coccolith as seen in distal view in transmitted light under the light microscope. D, Same coccolith seen in cross-polarized light (sample from Deep Sea Drilling Project [DSDP] Site 363, Core 8, section 2, 136 cm). E, Distal view of a coccolith as seen under the scanning electron microscope (SEM) (sample from ODP site 1218). The reticulum is fragile and easily dissolved. CA, central area; CO, central opening; DS, distal shield; PS, proximal shield.

any stratigraphic level and analyzing their change through time. Three characters yield meaningful biological and physiological information (Fig. 3):

1. Length of coccolith. In middle Eocene through early Miocene *Reticulofenestra* species, the coccolith size is linearly proportionate to cell size (Henderiks 2008), so the length of a coccolith constitutes a reliable proxy for the diameters of the cells and coccospheres. Thus, for example and regardless of geological age, a cell ~6 μm in diameter, can secrete several ~6-μm-long coccoliths and form a ~9 μm coccosphere (Supplementary Fig. S3). However, it is unknown whether there is a linear correlation between coccolith size and cell size (Henderiks 2008) for the large category (e.g., *R. umbilicus* and *R. hillae* in this study), as there are no data available for coccoliths larger than 10 μm.

2. Central opening/coccolith length ratio:

$$\text{Length ratio} = (\text{length of the central opening}/\text{length of the coccolith}) \times 100\%.$$

With a few exceptions, a central opening is present in all extinct/extant *Reticulofenestra* species, regardless of differences in the morphology of their shields. This strongly suggests that the role of the central opening is primordial and has remained unchanged along the *RGE* lineage.

3. Circularity of the coccolith:

$$\text{Circularity} = \text{width of coccolith}/\text{length of coccolith}.$$

Higher circularity means a more circular shape, while lower circularity means a more elliptical coccolith shape. Circularity reflects species diversity.

Statistical Analysis. To verify whether the observed morphologic variations between different stratigraphic intervals are significant, we applied analysis of variance (ANOVA) by grouping the samples into three groups (see details in the "Results"). Two different test methods were performed on the datasets. For the normally distributed datasets with similar variances, an ANOVA Tukey's pairwise post hoc test was applied. The Kruskal-Wallis and Mann-Whitney pairwise post hoc tests were used to test for equal means of nonnormally distributed datasets. The null hypothesis is that all the samples have the same mean values. If $p < 0.01$, then the hypothesis can be rejected, meaning that the tested datasets are significantly different. We added five samples, with 180 measurements in each, as replicates in the difference significance tests. The tests were conducted using PAST 4.06 (Hammer et al. 2001).

Age Model

The age model in this study is constrained by biostratigraphy. Data from calcareous nannofossil and planktonic foraminifera are consistent (Proto Decima et al. 1978; Toumarkine 1978; Keller 1983), and we verified the location of the calcareous nannofossil datums (Supplementary Fig. S4, Supplementary Table S1). We used the timescale of Gradstein et al. (2012).

The 100-m-thick section analyzed here represents an ~9 Myr interval, extending in terms of calcareous nannofossil biochronology from middle Eocene Biochron NP17 to early Oligocene Biochron NP23, with estimated ages of ~40 Ma and 31 Ma for the bounding horizons at ~212 and 114 mbsf. An age–depth plot (Supplementary Fig. S4) shows that the section is not temporally complete but includes several important hiatuses. The sediments across the Eocene/Oligocene boundary were eroded, with an inferred unconformity at ~186.6 mbsf (Core 9, section 3); the associated hiatus is ~0.9 Myr. Two additional unconformities truncate the middle to upper Eocene interval in Core 10. The oldest inferred unconformity at ~204.9 mbsf (in section 2) represents a ~2.8 Myr hiatus between ~37 and 39.8 Ma; the younger unconformity, at ~201 mbsf (top of Core 10), represents a ~2.1 Myr hiatus between 36.9 and 34.8 Ma. However, the lower Oligocene interval is continuous between ~187 and 109 mbsf (Cores 9 to 5), and was deposited at an estimated accumulation rate of 3.8 cm/kyr (Supplementary Fig. S4).

The discontinuous sedimentary record could hamper a comprehensive analysis of the evolution of *Reticulofenestra* through the late middle to late Eocene. However, the morphometric data show minor morphologic changes occurring from the middle through the late Eocene, although this interval is marked by long hiatuses in our section. Importantly, the FSR, which occurred in the early Oligocene (~32 Ma), is recorded in a demonstrably continuous stratigraphic interval (see Fig. 4). Further details can be found in Supplementary Fig. S4 and Supplementary Table S1.

Results

Variations in the Three Parameters

The coccolith length of *Reticulofenestra* between 212 and 114 mbsf at DSDP Site 363 comprises between ~3 and 20 μm, the central opening/coccolith length ratio between ~15% and 65%, and the circularity between 0.6 and 1 (Fig. 4A–C, small forms are in gray, and large forms are in orange). Based on size distribution, two size groups can be separated out at 9 μm (Fig. 5). Although there are substantial overlaps, the central opening/coccolith length ratio among the large forms is slightly higher than
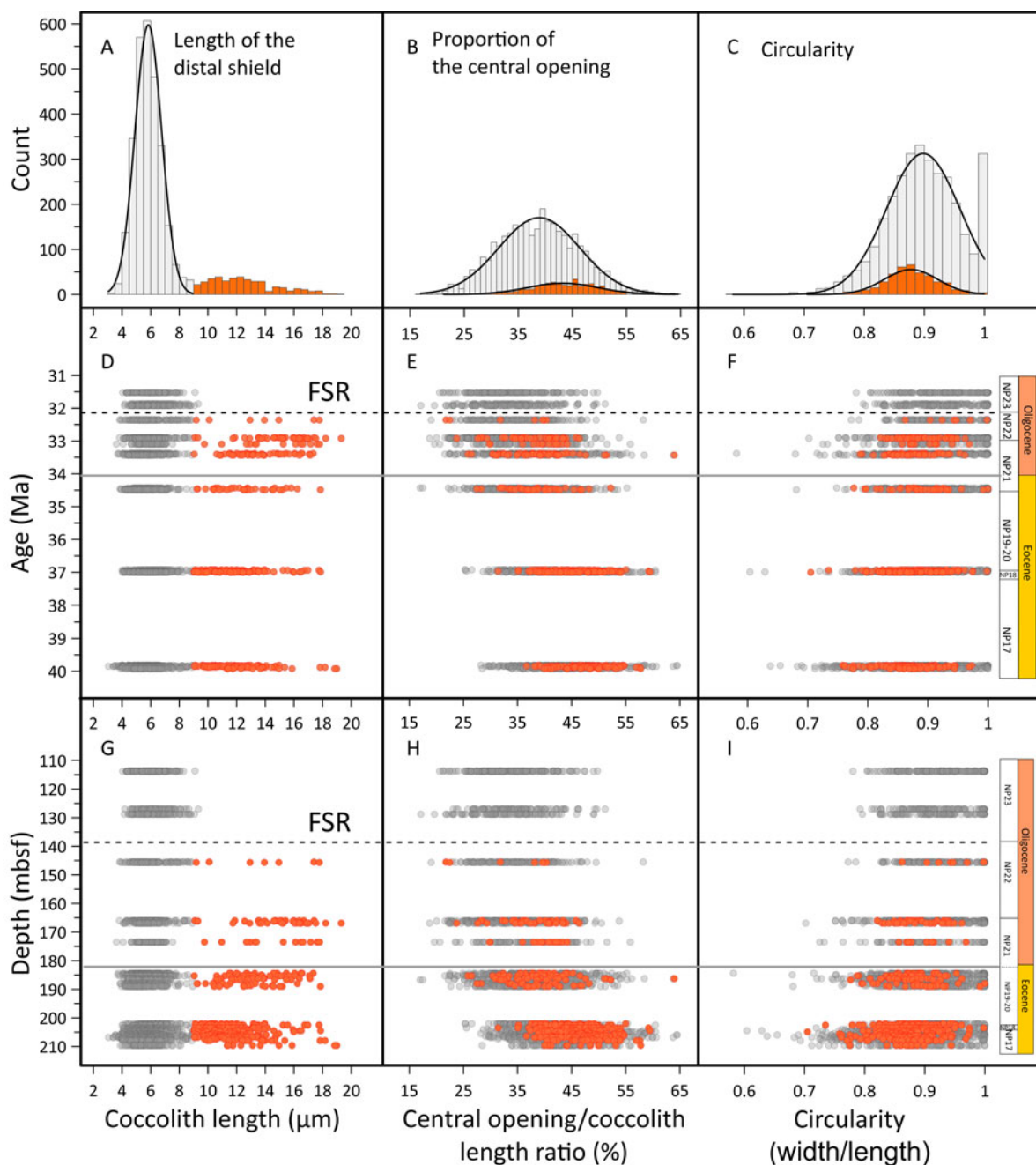
Figure 4. Distribution of the three morphologic characters analyzed in this study. A–C, Histograms with normal distribution fit. D–F, Distribution through time. G–I, Distribution through depth. Length of coccolith (A, D, G); coccolith width/length ratio (B, E, H); central opening/coccolith length ratio circularity (C, F, I). Dashed lines mark the first size reduction (FSR), while the gray lines indicate the Eocene/Oligocene boundary. The large group with coccolith length >9 μm is shown in orange histograms and scatters.

among the small to medium forms (Fig. 4B). All measured coccoliths range from long elliptical (<0.75) to circular (>0.98), although the most circular coccoliths (width/length = 1) are <9 μm in length (Fig. 4C). Eight species of *Reticulofenestra* were identified, of which 15 specimens were measured for each for comparison with the species' holotypes (Table 1). There is a structure to the morphologic variations, as shown by the integrated data, with three easily delineated intervals from the middle Eocene to lower Oligocene (Fig. 5).

The lower interval (Core 10, ~212 to 201 mbsf, middle Eocene Zone NP17 to lowermost upper Eocene Zone NP19-20, ~40–37

Ma; Fig. 5) is marked by contracted size distribution. Small to medium-sized coccoliths, ~3–9 μm long, dominate all assemblages, with the largest mean value of ~6.8 μm reached in the youngest stratigraphic level (~201 mbsf, NP18 zonal interval). Larger forms (coccolith length = 9–20 μm) occur consistently as well, although in notably smaller amounts. The central opening/coccolith length ratio varies from ~40% to 50% and markedly declines to ~38% at the top of this interval at ~201 mbsf (Fig. 5B). The broadest range in circularity (coccolith width/length) occurs in this interval, where minimal values of <0.6 and a mean value of 0.84–0.96 are recorded (Figs. 4, 5).
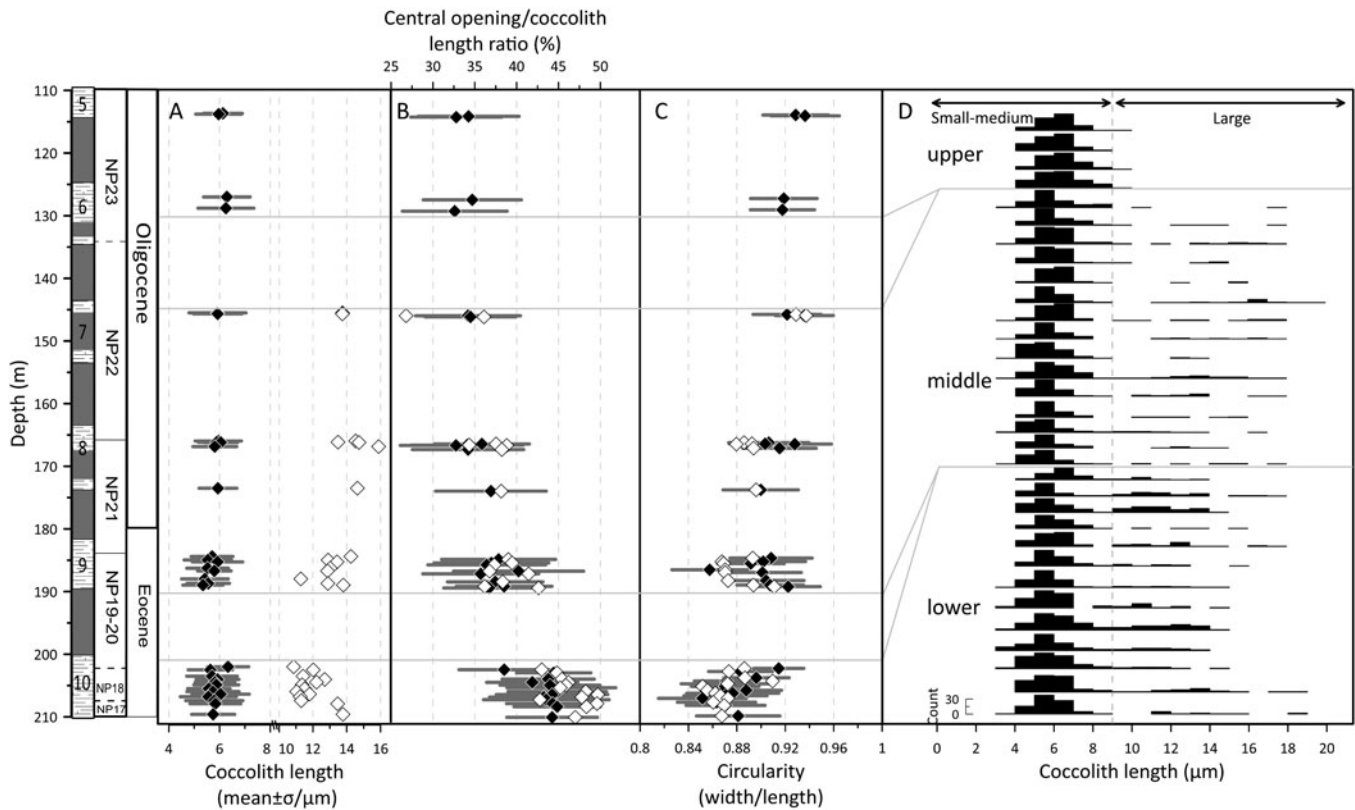
Figure 5. Results of the morphologic analysis of *Reticulofenestra* coccoliths. Large (>9 µm) and small to medium (≤9 µm) forms are shown in white and black rhombs, respectively. Standard deviations (gray bars) are shown in the small to medium forms. A, Coccolith length. B, Central opening/coccolith length ratio (%). C, Circularity of coccolith (width/length). D, Histograms of the length of the coccolith and distribution through depth. Vertical dashed line marks the size separation at 9 µm. Horizontal gray lines marks the three intervals.

Table 1. *Reticulofenestra* species identified in this study and size of selected characters of the holotypes as given in their original descriptions. CO is central opening/coccolith length ratio as measured on the attached photographs (Supplementary Plate S1).

Taxa	Length (mean ± σ/µm)	Holotype		
		Length (µm)	CO (%)	Reference
R. umbilicus	14.0 ± 2.3	16.1	41	Levin 1965
R. hillae	14.1 ± 1.4	14–20	27	Bukry and Percival 1971
R. coenura	10.4 ± 0.8	7–10	38	Roth 1970
R. nanggulanensis	6.0 ± 0.4	6	40	Jones and Dunkley Jones 2020
R. dictyoda	6.6 ± 0.6	5.6–6.6	27	Stradner and Edwards 1968
R. lockeri group	7.2 ± 0.6	7.6	42	Müller 1970
R. celticus	5.1 ± 0.3	4.8	41	Black 1962
R. floridana	7.5 ± 0.7	4.5–5	20	Hay et al. 1967
Reticulofenestra elliptical species	5.3 ± 0.5	—	—	—

In the middle interval (Cores 9–7, ~190–145 mbsf, upper Eocene Zone NP19-20 to lower Oligocene NP22, ~37–32.2 Ma; Fig. 5), coccoliths with lengths of ~3–9 µm are predominant, and larger forms are considerably fewer than in older stratigraphic levels. In addition, there is a progressive upward size increase (by ~4 µm) in the large forms (Fig. 4A,D,G). Also, the size continuum observed in the lower interval is disrupted in the upper part of this interval, where ~9-to 10-µm-long coccoliths are scarce. The central opening/coccolith length ratio decreases progressively from ~40%

to 35% on average, and the standard deviation in each sample is steady at ~5% (Fig. 5B). The circularity increases from ~0.9 to ~0.94 from the lower to the upper part of the interval, with one exceptionally low mean value occurring at ~187 mbsf (Fig. 5C).

There are no large forms (Figs. 4, 5) in the upper interval (Cores 6 and 5, ~130 to 114 mbsf, upper lower Oligocene Zone NP23, ~32.2–31.5 Ma; Fig. 5). The mean values of coccolith length are only ~5.6–5.7 µm, and the amplitude of variation (4–8 µm) of the coccolith length is more contracted than in

lower stratigraphic levels. In addition, this interval is characterized by the lowest central opening/coccolith length ratios (<35% on average; Fig. 5B) and the highest average circularity (>0.92; Fig. 5C) in the small- to medium-size group.

Significance Difference Test on the Three Parameters

Because the coccolith length does not follow a normal distribution, the Kruskal-Wallis and Mann-Whitney pairwise post hoc tests were used to test for the three intervals delineated. The results show that the lower (~40–37 Ma) and middle (~34.5–32.2 Ma) intervals differ significantly: a Kruskal-Wallis test for equal means shows $p(same) \leq 0.01$, and a Mann-Whitney test shows $p < 0.01$. The middle and the upper (~32.2–31.5 Ma) intervals show mathematically nonsignificant differences ($p > 0.05$), which is possibly due to the low abundance of the large forms in the middle interval. Nevertheless, from a micropaleontological perspective, these two intervals differ greatly, as the large forms (>9 μm) are absent from the upper interval, having disappeared at ~32.2 Ma. As the central opening/coccolith length ratio follows a normal distribution, a Tukey's pairwise test was conducted. It shows that the three intervals differ significantly ($p < 0.01$). For the circularity, the one-way analysis of similarities (ANOSIM) test also shows significant differences between the three intervals ($p < 0.01$).

Characterization of the FSR

The stratigraphic distribution of the coccolith length, central opening/coccolith length ratio, and circularity from the upper middle Eocene through the upper Oligocene unambiguously shows a major change in the size composition of the *Reticulofenestra* assemblages ~1.7 Myr after the Eocene/Oligocene boundary (Fig. 4). It is marked by the loss of coccoliths larger than 9 μm, together with a narrowing of the amplitude of variation of both the central opening/coccolith length ratio and the circularity (Fig. 5B,C). Before the FSR (~32 Ma), small- to medium-sized coccoliths (~3–9 μm) dominated the assemblages, and larger coccoliths (~9–-20 μm) were consistently present, even though their number decreased through time. Above the NP22/NP23 boundary, these large coccoliths had disappeared, and at the same time, the size variations of the small to medium coccoliths had become more restricted and the length of the central opening had decreased. The FSR describes this early Oligocene biotic event, dated at ~32.2 Ma based on our age model, which affected the size of *Reticulofenestra* coccoliths. On this basis, we infer that the FSR also describes a considerable reduction in the cell/coccosphere size of *Reticulofenestra* species.

Discussion

Collective Adaptive Morphology of the *Reticulofenestra* Species during the FSR

As highlighted in this study of Site 363, until 32.3 Ma, the late middle Eocene to early Oligocene, *Reticulofenestra* coccoliths were segregated into two main size categories, with small- and medium-size coccoliths distinct from larger forms (Fig. 6). One category, rather stable, consisted of small- to medium-sized
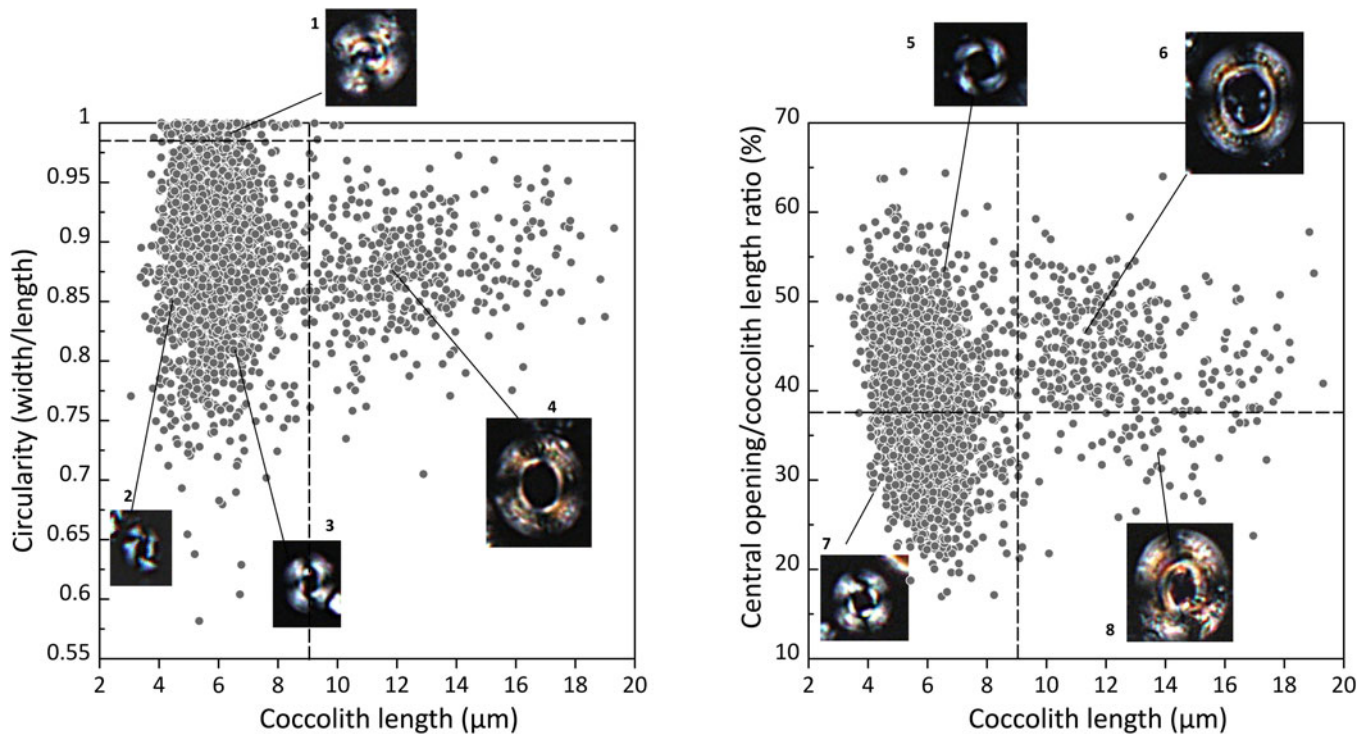

Figure 6. Comparison between morphometric characters of the late middle Eocene through early Oligocene *Reticulofenestra* coccoliths at Deep Sea Drilling Project (DSDP) Site 363. All measurements are incorporated in this figure. Dashed lines separate different morphotypes based on each parameter (two size groups are separated by coccolith length = 9 μm; circular group is characterized by the coccolith circularity > 0.98; central opening/coccolith length ratio = 38% separates small-large central opening). Images are from the study material. 1, *Reticulofenestra floridana*; 2, *Reticulofenestra* sp.; 3, *Reticulofenestra dictyoda*; 4, *Reticulofenestra umbilicus*; 5, *Reticulofenestra nanggulanensis*; 6, *R. umbilicus*; 7, *R. dictyoda*; 8, *Reticulofenestra hillae* (detailed in R.M. and M.-P.A., unpublished data).

coccoliths with a mean length of ~6 μm, a 15–60% central opening/coccolith length ratio, and ~0.70 to 1.00 in circularity; the other category ranged from ~9 to 20 μm in length, 25% to 55% in the central opening/coccolith length ratio, and ~0.80 to 0.95 in circularity. These marked differences imply the existence of two groups of species, possibly with different environmental preferences, as often seen in the species of the *RGE* lineage (e.g., Hagino et al. 2000; Beaufort and Heussner 2001) and extinct *Reticulofenestra* (e.g., Imai et al. 2015).

The diversity of the small- to medium-sized coccoliths was driven by a broad range in the central opening/coccolith length ratio and circularity. The central opening/coccolith length ratio decreased from the late middle Eocene through the early Oligocene, while the abundance of circular coccoliths increased. The important moment in this transition was near the NP18/NP19-20 biochronal boundary (~37 Ma), immediately after which the central opening/coccolith length ratio had shifted from ~45% (before) to ~36%, and when a minimum circularity of 0.84–0.9 was reached. This was reflected by a notable increase in circular *Reticulofenestra* coccoliths with a small central opening across the Eocene/Oligocene transition (see also Wei and Wise 1990; Dunkley Jones et al. 2008). To explain this evolutionary history, we hypothesize that during the middle to early late Eocene (Biochron NP17 to early Biochron NP19-20, 40–34.5 Ma), the surface ocean was populated by species bearing coccoliths of diverse ellipticity with a central area opened to varying degrees. By ~34.5 Ma (late Biochron NP19-20), the proportion of species bearing (sub)circular coccoliths with a small central opening had increased. These achieved dominance in the early Oligocene (Biochron NP22), a dominance they maintained through Biochron NP23.

The large (>9 μm) *Reticulofenestra* coccoliths underwent a different evolutionary history. They form a diverse category of subcircular to broadly elliptical coccoliths, most with a large central area (>25%). The abundance and mean size of this category were rather constant during Biochrons NP17 and NP18. This constancy suggests a stable ecological niche. In contrast, from Biochron NP19-20 to Biochron NP22, the abundance of these large species decreased steadily at the same time as the length of their coccoliths (and by implication, the diameter of the cells) increased, indicating that the ecological niche might have begun to change. This decrease in abundance concomitant with an increase in cell size continued until the end of Biochron NP22, when a shift toward dominance of the larger species (~18 μm in cell diameter) with a smaller central opening (<35%) occurred in *Reticulofenestra hillae*, which suggests a broadening of the habitat to adapt to changing environments. The extinction of all the large species followed, which is the most visible component of the FSR.

In summary, as recognized through morphologic analysis of coccoliths and broadly converting these data into cell size, the late middle Eocene through early Oligocene evolutionary history of *Reticulofenestra* species reveals two distinct strategies leading to the FSR. Species with cells of small to medium size maintained a constant mean size, although their total size became greatly constrained after the FSR at the same time as species with circular placoliths and small central openings became dominant. In contrast, the species with large cells decreased in abundance at the same time as their mean diameter increased. The strategic divergence between the two size groups of species probably began in the late Eocene, increasing progressively during the early Oligocene to reach a maximum immediately before the FSR.

The FSR is thus a complex event that involved different responses of the *Reticulofenestra* species depending on cell size.

Climatic Forcing on Size Evolution of Coccolithophores of the RGE Lineage

Although the ecology of individual species of living coccolithophores remains poorly known, a general understanding of the relationship between cell size and physiology or ecology is emerging (Linnert and Mutterlose 2015; Sheward et al. 2017; Faucher et al. 2020; Beaufort et al. 2021). Geographic distribution and temporal evolution indicate that different size groups (morphotypes) can have specific depth or seasonal niches (e.g., Beaufort and Heussner 2001; Suchéras-Marx et al. 2010), while culture studies have shown that environmental factors, including temperature, light, carbon dioxide (CO_2), and nutrients, have a significant control on cell size (e.g., Müller et al. 2008; Aloisi 2015).

It is difficult to constrain a driving mechanism for coccolith/cell size evolution from fossil records because of the multiple environmental factors involved. However, the long-term size adaptation of the coccolithophores during the Cenozoic is currently attributed to long-term changes in atmospheric pCO$_2$ (e.g., Henderiks and Pagani 2008; Erba et al. 2010; Hannisdal et al. 2012; Bordiga et al. 2015; Guitián et al. 2020; Henderiks et al. 2020). Atmospheric pCO$_2$ is regarded as a main evolutionary driver, because the lower volume/surface area ratio (V:SA) of large cells is seen as a weakness for the uptake of carbon resources, which leads to a failure in survival in low pCO$_2$ conditions (Henderiks and Pagani 2008). The threshold behavior of the atmospheric pCO$_2$ found to be responsible for the Antarctic glaciation and the Eocene–Oligocene global climate transition (DeConto and Pollard 2003; Pearson et al. 2009; Hutchinson et al. 2021) could account for the evolutionary events across this transition, as described here. In addition, the occurrence of large *Reticulofenestra* during the middle Eocene (~40 Ma; Backmann and Hermelin 1986), when atmospheric pCO$_2$ levels were at the highest of the late Paleogene (Rae et al. 2021), would seem to support a long-term control of pCO$_2$ on the coccolithophore size. The relationship between coccolith size and pCO$_2$, however, is not a simple one. A short-term control is, in fact, not easily applicable to the rapid evolution of *Reticulofenestra* size during the Neogene, when repeated size divergences and extinctions occurred without considerable fluctuations in CO_2 concentrations (e.g., Young 1990; Gibbs et al. 2005; Imai et al. 2015). More importantly, Quaternary fossil records have shown that the large species in the *RGE* lineage always become larger and reach a size maximum before their extinctions (e.g., Matsuoka and Okada 1990). The so-called Matsuoka and Okada cycle (Bendif et al. 2019) refers to very typical evolutionary pattern that is also seen in the Neogene (e.g., Young 1990; Imai et al. 2015) and Paleogene *Reticulofenestra* (this study; Fig. 5D). The pre-extinction size increases may represent the initiation of each recurring evolutionary event. However, these events are not always synchronous with CO_2 variations. Our data show that the changes in morphology and abundance patterns of *Reticulofenestra* species between ~40 and 31 Ma were not synchronous with pCO$_2$ changes (Fig. 7). Substantial morphologic changes in *Reticulofenestra* species, including enlargement of the larger cells and a ~10% decrease in the central opening of all coccoliths, began ~2–3 Myr earlier than the distinct drop in pCO$_2$ in the earliest Oligocene (Pagani et al. 2011; Zhang et al. 2013; Anagnostou et al. 2020; Fig. 7). It would seem, therefore,
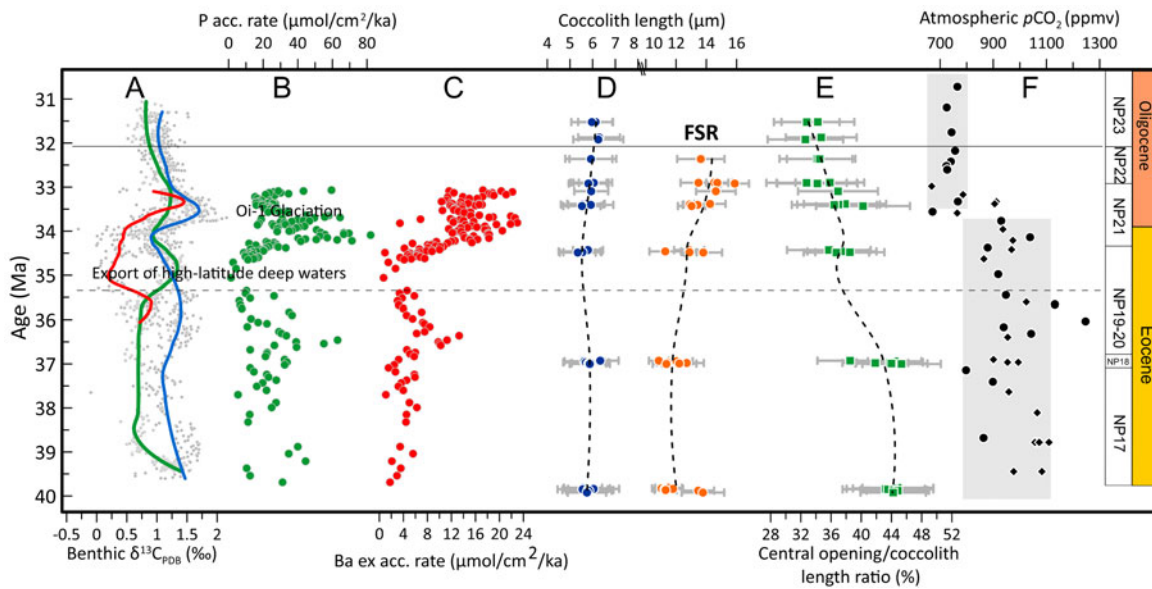
Figure 7. Integration of morphologic changes in *Reticulofenestra* at Deep Sea Drilling Project (DSDP) Site 363 and paleoceanographic records during the late middle Eocene through the early Oligocene (40–31 Ma). A, Stable carbon isotopic records from the middle latitude South Atlantic Ocean (Ocean Drilling Program Site 1263, ~2100 m, blue line; Langton et al. 2016), sub-Antarctic South Atlantic Ocean (ODP 1090, ~3200 m, red line; Pusz et al. 2011), and Southern Ocean (ODP 689, ~1400 m, green line; Diester-Haass and Zahn 1996). B, C, Total phosphorus and extra barium accumulation rates (Anderson and Delaney 2005). D, Average size of the medium-small (blue circles, coccolith length ≤ 9 μm) and the large (orange circles, coccolith length > 9 μm) *Reticulofenestra* coccoliths. E, Average central opening/coccolith length ratio for all *Reticulofenestra* coccoliths. F, Proxy reconstructions of the atmospheric pCO_2 (circle: Zhang et al. 2013; rhombus: Anagnostou et al. 2020). Note that a single pCO_2 data point with a value of 2622 ppm at ~36.5 Ma in Zhang et al. (2013) is not shown. Dashed lines in B, C, and D are LOESS smoothed.

that an additional forcing is involved in the size evolution of the *RGE* lineage. We propose that nutrient concentration in the upper ocean was that forcing.

Studies of cores from different oceans at different latitudes show that coccolithophores responded to the global nutrient concentration increases during the Eocene/Oligocene transition, as the (inferred) oligotrophic taxa were vastly replaced by (inferred) eutrophic taxa (Dunkley Jones et al. 2008; Villa et al. 2014, 2021; Bordiga et al. 2015; Jones et al. 2019). The changes in coccolith length and central opening/coccolith length ratio that we describe here from Site 363 on the Frio Ridge portion of the Walvis Ridge were synchronous with increased nutrient availability and productivity during the late Eocene and early Oligocene (~34.5–32 Ma), as determined from proxy-reconstructed nutrient concentration (P accumulation rate) and export productivity (biogenic Ba) in the South Atlantic Ocean (Anderson and Delaney 2005) (Fig. 7D,E). Micropaleontologic/paleoceanographic studies have proposed that smaller *Reticulofenestra* are better adapted to upwelling and nutrient-rich conditions (Bolton et al. 2010; Imai et al. 2015) or simply to more dynamic environments (Holcová 2013). During the late Eocene, DSDP Site 363 underwent intensified surface- and deep-water circulation (Corliss et al. 1984). This was likely related to the deep-sea overturning circulation established during the same time, bringing Antarctic Intermediate Water (AAIW) into the southern Atlantic Ocean at mid- to low latitudes (Katz et al. 2011; Egan et al. 2013; Coxall et al. 2018; Fig. 7A). Early Oligocene overturning circulation meant a worldwide expansion of oceanic eutrophy at the expense of oligotrophy. The upwelling system in the eastern South Atlantic Gyre that was sustained by the Benguela Current (Lutjeharms and Meewis 1987) may be the dynamic that brought nutrients from the AAIW (~750 m; Sarmiento et al. 2004; Katz et al. 2011) to the surface ocean during the early Oligocene. On this basis, it can

be speculated that the increase in small *Reticulofenestra* cells indicates the expansion of oceanic eutrophic conditions, while the extinction of large cells indicates the reduction/loss of oligotrophic conditions (Fig. 7). The synchronous decrease in the central opening of the coccoliths (Fig. 7D,E) may also be the result of ocean eutrophication, which is worth exploring from the perspective of adaptive morphology.

Adaptive Morphology in the RGE Lineage

Previous studies dealing with forcing on *Reticulofenestra* evolution have centered on the size of coccoliths and cells, often ignoring the shape of the former (e.g., Beaufort 1992; Gibbs et al. 2005; Henderiks and Pagani 2008; Imai et al. 2015; Guitián et al. 2020), although theoretically adaptive morphology is important (Aubry 2007). An exception concerns the study by Backman and Hermelin (1986), who calculated the ratio of the diameter of the central opening to the length of the coccolith. They showed a progressive decline in the central opening/coccolith length ratio in the large forms during the middle to late Eocene, and attributed it to a simultaneous oceanic cooling documented by Shackleton (1975). Our study confirms the finding by these authors that the size of the central opening is as important as the length of the coccoliths in describing morphologic evolution in *Reticulofenestra*.

Like the living species of the *RGE* lineage (see www.mikrotax.org/Nannotax3), the coccospheres of *Reticulofenestra* species would have consisted of interlocking coccoliths with small gaps between them allowing contact between seawater and the cell itself. It may be inferred that in species possessing coccoliths with no or tiny central openings, the surface area (and volume) represented by the gaps was much greater than the surface (volume) represented by the central openings, as can be seen in the

recently extinct *Gephyrocapsa caribbeanica* Boudreaux and Hay, 1967 in Hay et al. 1967. In contrast, in species possessing coccoliths with a large central opening, the surface (volume) represented by the openings would have exceeded the surface (volume) represented by the gaps and would have markedly increased the porosity of the coccosphere (as can be seen in the living species *Gephyrocapsa oceanica* Kamptner, 1943). By inference, the central opening in the large *Reticulofenestra* species of the FSR would have been a primary contact between the cell and its environment. It is important to recognize that a thin, organic, pattern-less base plate likely underlined the proximal side of the *Reticulofenestra* coccoliths, as in *Emiliania huxleyi* (Billard and Inouye 2004). Such a base plate is seen to constitute a physical barrier below the central opening and its perforated proximal grid. However, in the absence of evidence to the contrary, and considering its reactivity during intracellular calcification (Paasche 2001; Marzec et al. 2019), it may be speculated that the base plate in the *RGE* lineage may not have constituted a chemical barrier to nutrients penetrating the cell through the central opening.

In small as in large *Reticulofenestra* coccoliths, the diameter of the perforations (as measured on scanning electron microscope (SEM) images of *Reticulofenestra umbilicus*, *Reticulofenestra lockeri*, *Reticulofenestra dictyoda*, etc. available on Nannotax3) of the proximal grid across the central opening is almost constant (~0.2 μm), which implies that the pores (and the central opening) have a very specific function (Fig. 3). We concur with Young (1987), who, noting the ubiquity of perforations in coccoliths of extinct and living species, inferred a physiologic role for them in interactions between the cell and seawater. Although this speculation is technically difficult to prove, there is support from both environmental and laboratory studies. For instance, Hagino et al. (2000) observed that in the modern equatorial Pacific Ocean, the morphotypes of *Gephyrocapsa* with a wide central opening were better adapted to a more stable environment and nutrient-poor conditions. Bartal et al. (2015) found that the coccospheres of *E. huxleyi* provide stable, enclosed microenvironments that benefit cells during the uptake of nutrients in turbulent water columns. This may be interpreted by analogy with studies of the role of a skeleton in diatoms. For example, using numerical modeling, Mitchell et al. (2013) suggested that when pulses of water pass the cells, nutrient concentration equilibrates quickly. Then, the closed surface structure of the skeleton produces asymmetric diffusion resistance. The highly limited out-diffusion from the cell to the surrounding waters permits the retention of a high nutrient concentration surrounding the membrane (Mitchell et al. 2013), which is essential for nonmotile unicellular organisms (Falkowski and Oliver 2007). We hypothesize that the coccosphere had a similar function in modulating nutrient transport, the smaller central opening being beneficial for coccolithophores' autotrophic nutrient uptake, especially in turbulent water.

In contrast, our data suggest that large species with broadly open coccoliths were better adapted to the oligotrophic ocean. A possible explanation is that larger openings facilitated nutrient uptake through mixotrophy. Autotrophy has been seen as the rule among coccolithophores, but mixotrophy has been speculated based on morphologic/structural analysis of coccoliths and coccospheres (Aubry 2009; Young et al. 2009; Gibbs et al. 2020), and there is increasing experimental and field evidence that this may be the case. Coccolithophores are able to both prey on (e.g., Parke and Adams 1960; Rokitta 2011; Avrahami and Frada 2020) and absorb (e.g., Benner and Passow 2010;

Godrijan et al. 2020, 2022) organic components from the environment. In fact, it is now recognized that mixotrophy, as an intermediate physiology between autotrophy and heterotrophy, occurs in all ecosystems and across the whole eukaryotic phylogeny (Selosse et al. 2017). The cell of planktonic algae is surrounded by a zone enriched in its discarded metabolic products. These attract bacteria, which contribute their own metabolic components, some of which can in turn be used as nutrients by the algae (Smriga et al. 2016; Seymour et al. 2017). This beneficial dual strategy is embodied in the tentative concept of a phycosphere (Bell and Mitchell 1972; Liu et al. 2022), and Seymour et al. (2017) have suggested that the degree of symbiotic mixotrophy in *E. huxleyi* can be determined by the size of the phycosphere where diffused organic matter is utilized via bacterial chemotaxis. We hypothesize, therefore, that a large central opening, allowing enhanced plankton–bacteria interactions, may have favored mixotrophic activities in the oligotrophic ocean of the Eocene.

At present, the oligotrophic upper photic zone is inhabited by large, usually K-selected species (Hagino et al. 2000; Kinkel et al. 2000). By comparison, we suggest that while the small to medium *Reticulofenestra* were r-selected species and lived in more eutrophic waters, the large *Reticulofenestra* species were K-selected and inhabited oligotrophic environments (Fig. 8).

To summarize, we propose an ecological model that relates nutrient forcing to morphology in *Reticulofenestra* (Fig. 9).
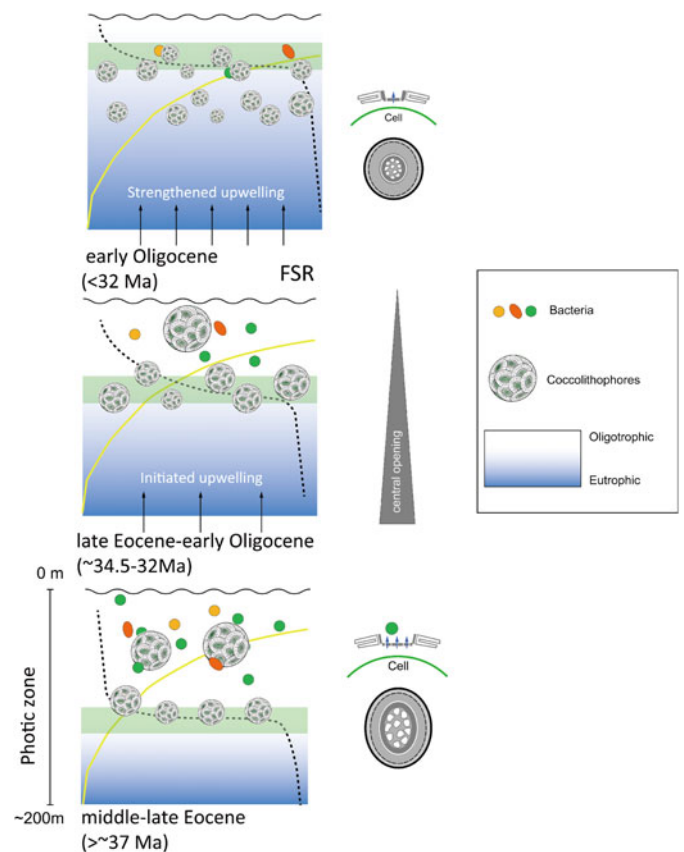

Figure 8. Interpretation of the *Reticulofesnestra* response to environmental forcing from the late middle Eocene to early Oligocene and relevance to the first size reduction (FSR). The green layer marks the depth of the nutricline. The yellow curve and black dashed line represent the light intensity and the nutrient concentration, respectively. The gray triangle indicates the decreasing diameter of the central opening.
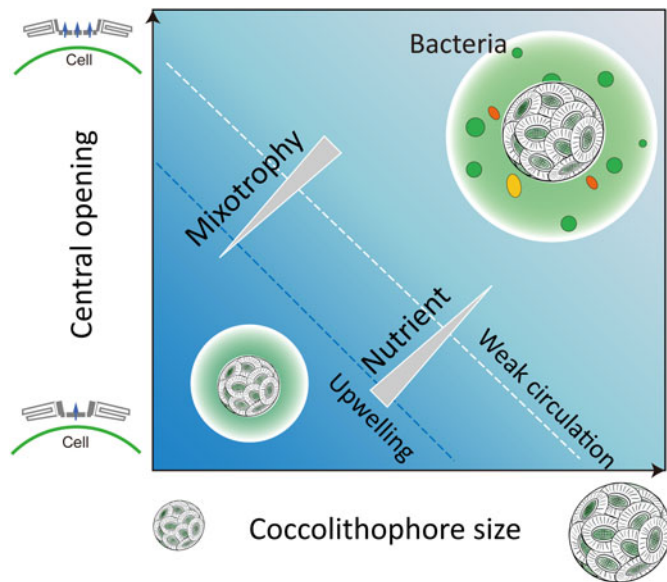
Figure 9. Hypothetical ecological model for coccolithophores of the *RGE* lineage. Cells with coccospheres consisting of small- to medium-size coccoliths with a narrow central area characterize species that live in eutrophic conditions; their phycosphere is slight, and they rely little on mixotrophy. Larger cells possessing coccospheres consisting of large coccoliths with a wide, central opening lived in oligotrophic conditions; their phycosphere was voluminous and they strongly relied on mixotrophy. The greenish area surrounding the coccospheres represents the phycosphere.

Species with different cell sizes and lengths of the central openings of their coccoliths adapted differently to varying degrees of nutrient availability. The larger species with a large central opening that would have facilitated mixotrophy were better adapted to the warm, oligotrophic ocean; smaller species with a smaller central opening were better adapted to the eutrophic ocean, where they depended less on mixotrophy. This tentative model explains the divergent adaptive morphology of *Reticulofenestra* species around the Eocene/Oligocene transition, and it may help in conceptualizing changes in coccolith morphology in the *RGE* lineage through time in terms of adaptive evolution in an evolving ocean.

Conclusions

The sudden disappearance of large *Reticulofenestra* species from the early Oligocene coccolithophore communities has been known for a long time (Martini 1971; Backman and Hermelin 1986). We term it the "first size reduction" (FSR, ~32 Ma) of the *Reticulofenestra-Gephyrocapsa-Emiliania* (*RGE*) lineage and describe it quantitatively in the double context of the long-term (~40–31 Ma) morphologic history of the coccoliths of this lineage and the important paleoceanographic changes that were associated with global cooling, Antarctic glaciation, and atmospheric pCO$_2$ decline during the Eocene/Oligocene transition (Zachos et al. 1996; Coxall and Wilson 2011). We show that the decrease in pCO$_2$ postdates by ~2–3 Myr the first indication of destabilization of size structure among late Eocene *Reticulofenestra* communities. All *Reticulofenestra* species, small and large, were simultaneously affected by progressive establishment of global oceanic eutrophication starting in the late Eocene, although their response in terms of adaptive morphology varied with coccolith length. The larger species (>9 μm) became extinct at the FSR, ~3–5 Myr after the first evidence of destabilization of the *Reticulofenestra* community, and we hypothesize that this

extinction reflected the disappearance of a warm oligotrophic surface ocean. From this, we infer that the large FSR *Reticulofenestra* species were K-selected and with ecological requirements like those of extant coccolithophores with large coccoliths. In this scenario, these *Reticulofenestra* species, which consistently possessed coccoliths with wide central openings, relied on absorbotrophic mixotrophy via interactions with bacteria living in the nutrient-enriched waters immediately surrounding the coccosphere. By contrast, the smaller species (≤9 μm) flourished after the FSR, when the relative size of the central opening of the coccoliths decreased. We infer that these species, dominated by *Reticulofenestra floridana*, were r-selected and adapted to the more eutrophic surface waters that would have prevailed after the FSR. We propose that the reduction in the central opening/coccolith length ratio was an adaptation to these more eutrophic conditions, suggesting that mixotrophy was not favored for the duration of Biochron NP23 (~32–30 Ma), when coccolithophore diversity was at its lowest level of the Paleogene (Aubry 1992).

We add nutrient availability in the photic zone to variations in atmospheric pCO$_2$ to account for the long-term evolution of size in the coccolithophores. This is not to claim that pCO$_2$ has played no evolutionary role. We propose, however, that the adaptive morphology of coccoliths, not only cell size, should be considered to decipher the long- (and short-) term evolution of the species of the *RGE* lineage, and of coccolithophores in general. Our interpretation also echoes the view that the diversity of trophic strategies among coccolithophores is vastly underestimated (Segev et al. 2016; Taylor et al. 2017; Godrijan et al. 2020, 2022; Henderiks et al. 2022) and that this diversity underpins the biodiversity of coccolithophores.

Literature Cited

Agnini, C., G. Muttoni, D. V. Kent, and D. Rio. 2006. Eocene biostratigraphy and magnetic stratigraphy from Possagno, Italy: the calcareous nannofossil response to climate variability. *Earth and Planetary Science Letters* **241**:815–830.

Agnini, C., I. Raffi, J. Backman, E. Fornaciari, D. Rio, and H. Pälike. 2014. A new low- to middle-latitude biozonation and revised biochronology of Palaeogene Calcareous nannofossils. *Newsletters on Stratigraphy* **47**:131–181.

Aloisi, G. 2015. Covariation of metabolic rates and cell size in coccolithophores. *Biogeosciences* **12**:4665–4692.

Anagnostou, E., E. H. John, T. L. Babila, P. F. Sexton, A. Ridgwell, D. J. Lunt, P. N. Pearson, T. B. Chalk, R. D. Pancost, and G. L. Foster. 2020. Proxy evidence for state-dependence of climate sensitivity in the Eocene greenhouse. *Nature Communications* **11**:4436.

Anderson, L. D., and M. L. Delaney. 2005. Middle Eocene to early Oligocene paleoceanography from Agulhas Ridge, Southern Ocean (Ocean Drilling Program Leg 177, Site 1090). *Paleoceanography* **20**(1). https://doi.org/10.1029/2004PA001043.

Avrahami, Y., and M. J. Frada. 2020. Detection of phagotrophy in the marine phytoplankton group of the coccolithophores (Calcihaptophycidae, Haptophyta) during nutrient-replete and phosphate-limited growth. *Journal of Phycology* **56**:1103–1108.

Aubry, M.-P. 1992. Late Paleogene calcareous nannoplankton evolution: a tale of climatic deterioration. Pp. 272–309 in D. Prothero and W. Berggren, eds. *Eocene-Oligocene climatic and biotic evolution*. Princeton University Press, Princeton, N.J.

Aubry, M.-P. 2007. A major Pliocene coccolithophore turnover: change in morphological strategy in the photic zone. *Geological Society of America Special Paper* **424**:25–51.

Aubry, M.-P. 2009. A sea of Lilliputians. *Palaeogeography, Palaeoclimatology, Palaeoecology* **284**:88–113.

Aubry, M.-P., and D. Bord. 2009. Reshuffling the cards in the photic zone at the Eocene/Oligocene boundary. The Late Eocene Earth—hothouse, icehouse, and impacts. *Geological Society of America Special Paper* **452**:279–301.

Backman, J., and J. O. R. Hermelin. 1986. Morphometry of the Eocene nannofossil *Reticulofenestra umbilicus* lineage and its biochronological consequences. *Palaeogeography, Palaeoclimatology, Palaeoecology* **57**:103–116.

Backman, J., I. Raffi, D. Rio, E. Fornaciari, and H. Pälike. 2012. Biozonation and biochronology of Miocene through Pleistocene calcareous nannofossils from low and middle latitudes. *Newsletters on Stratigraphy* **45**:221–244.

Bartal, R., B. Shi, W. P. Cochlan, and E. J. Carpenter. 2015. A model system elucidating calcification functions in the prymnesiophyte *Emiliania huxleyi* reveals dependence of nitrate acquisition on coccoliths. *Limnology and Oceanography* **60**:149–158.

Beaufort, L. 1992. Size variations in Late Miocene *Reticulofenestra* and implication for paleo climatic interpretation. *Memorie di Scienze Geologiche, Universita di Padova* **7**:339–350.

Beaufort, L., and S. Heussner. 2001. Seasonal dynamics of calcareous nannoplankton on a West European continental margin: the Bay of Biscay. *Marine Micropaleontology* **43**:27–55.

Beaufort, L., C. T. Bolton, A.-C. Sarr, B. Suchéras-Marx, Y. Rosenthal, Y. Donnadieu, N. Barbarin, S. Bova, P. Cornuault, Y. Gally, E. Gray, J.-C. Mazur, and M. Tetard. 2021. Cyclic evolution of phytoplankton forced by changes in tropical seasonality. *Nature* **476**:80–84.

Bell, W., and R. Mitchell. 1972. Chemotactic and growth responses of marine bacteria to algal extracellular products. *Biological Bulletin* **143**:265–277.

Bendif, E. M., B. Nevado, E. L. Y. Wong, K. Hagino, I. Probert, J. R. Young, R. E. M. Rickaby, and D. A. Filatov. 2019. Repeated species radiations in the recent evolution of the key marine phytoplankton lineage *Gephyrocapsa*. *Nature Communications* **10**:4234.

Benner, I., and U. Passow. 2010. Utilization of organic nutrients by coccolithophores. *Marine Ecology Progress Series* **404**:21–29.

Billard, C., and I. Inouye. 2004. What is new in coccolithophore biology? Pp. 1–30 in H. R. Thierstein and J. Young, eds. *Coccolithophores—from molecular processes to global impact*. Springer, Berlin.

Black, M. 1962. Fossil coccospheres from a Tertiary outcrop on the continental slope. *Geological Magazine* **99**:123–127.

Bolli, H., W. Ryan, J. Foresman, W. Hottman, H. Kagami, J. Longoria, B.K. McKnight et al. 1978. Walvis Ridge—sites 362 and 363. Vol. **40**, Pp. 183–356 in H. M. Bolli, W. B. F. Ryan, J. B. Foresman, W. E. Hottman, H. Kagami, J. F. Longoria, B. K. McKnight, et al. *Initial Reports of the Deep Sea Drilling Project*. Texas A&M University, Ocean Drilling Program, College Station, Tex.

Bolton, C. T., K. T. Lawrence, S. J. Gibbs, P. A. Wilson, L. C. Cleaveland, and T. D. Herbert. 2010. Glacial–interglacial productivity changes recorded by alkenones and microfossils in late Pliocene eastern equatorial Pacific and Atlantic upwelling zones. *Earth and Planetary Science Letters* **295**:401–411.

Bordiga, M., J. Henderiks, F. Tori, S. Monechi, R. Fenero, A. Legarda-Lisarri, and E. Thomas. 2015. Microfossil evidence for trophic changes during the Eocene–Oligocene transition in the South Atlantic (ODP Site 1263, Walvis Ridge). *Climate of the Past* **11**:1249–1270.

Bown, P. R., J. A. Lees, and J. R. Young. 2004. Calcareous nannoplankton evolution and diversity through time. Pp. 481–508 in H. R. Thierstein and J. R. Young, eds. *Coccolithophores*. Springer, Berlin.

Bukry, D., and S. F. Percival. 1971. New Tertiary calcareous nannofossils. *Tulane Studies in Geology and Paleontology* **8**:123–146.

Corliss, B. H., M.-P. Aubry, W. Berggren, J. M. Fenner, L. D. Keigwin, and G. Keller. 1984. The Eocene/Oligocene boundary event in the deep sea. *Science* **226**:806–810.

Coxall, H. K., and P. A. Wilson. 2011. Early Oligocene glaciation and productivity in the eastern equatorial Pacific: insights into global carbon cycling. *Paleoceanography* **26**:1–18.

Coxall, H. K., C. E. Huck, M. Huber, C. H. Lear, A. Legarda-Lisarri, M. O'Regan, K. K. Sliwinska, T. van de Flierdt, A. M. de Boer, J. C. Zachos, and J. Backman. 2018. Export of nutrient rich Northern Component Water preceded early Oligocene Antarctic glaciation. *Nature Geoscience* **11**:190–196.

DeConto, R. M., and D. Pollard. 2003. Rapid Cenozoic glaciation of Antarctica induced by declining atmospheric CO_2. *Nature* **421**:245–249.

Diester-Haass, L., and R. Zahn. 1996. Eocene–Oligocene transition in the Southern Ocean: history of water mass circulation and biological productivity. *Geology* **24**:163–166.

Driever, B. W. M. 1988. Calcareous nannofossil biostratigraphy and paleoenvironmental interpretation of the Mediterranean Pliocene. *Utrecht Micropaleontological Bulletin* **36**:1–245.

Dunkley Jones, T., P. R. Bown, P. N. Pearson, B. S. Wade, H. K. Coxall, and C. H. Lear. 2008. Major shifts in calcareous phytoplankton assemblages through the Eocene–Oligocene transition of Tanzania and their implications for low-latitude primary production. *Paleoceanography* **23**:PA4204.

Egan, K. E., R. E. M. Rickaby, K. R. Hendry, and A. N. Halliday. 2013. Opening the gateways for diatoms primes Earth for Antarctic glaciation. *Earth and Planetary Science Letters* **375**:34–43.

Erba, E., C. Bottini, H.J. Weissert and C. E. Keller. 2010. Calcareous nannoplankton response to surface-water acidification around Oceanic Anoxic Event 1a. *Science* **329**:428–432.

Falkowski, P. G., and M. J. Oliver. 2007. Mix and match: how climate selects phytoplankton. *Nature Reviews Microbiology* **5**:813–819.

Faucher, G., U. Riebesell and L. T. Bach, L. T. 2020. Can morphological features of coccolithophores serve as a reliable proxy to reconstruct environmental conditions of the past? *Climate of the Past* **16**:1007–1025.

Gallagher, L. 1989. *Reticulofenestra*: a critical review of taxonomy and evolution. Pp. 41–75 in J. Crux and S. E. van Heck, eds. *Nannofossils and their applications: Proceedings of the Second International Nannoplankton Association Symposium*, London. Ellis Horwood, Chichester, U.K.

Gibbs, S. J., J. R. Young, T. J. Bralower, and N. J. Shackleton. 2005. Nannofossil evolutionary events in the mid-Pliocene: an assessment of the degree of synchrony in the extinctions of *Reticulofenestra pseudoumbilicus* and *Sphenolithus abies*. *Palaeogeography, Palaeoclimatology, Palaeoecology* **217**:155–172.

Gibbs, S. J., P. R. Bown, B. A. Ward, S. A. Alvarez, H. Kim, O. A. Archontikis, O. A. Odysseas, B. Sauterey, A. J. Poulton, J. Wilson, and A. Ridgwell. 2020. Algal plankton turn to hunting to survive and recover from end-Cretaceous impact darkness. *Science Advances* **6**: eabc9123.

Godrijan, J., D. Drapeau, and W. M. Balch. 2020. Mixotrophic uptake of organic compounds by coccolithophores. *Limnology and Oceanography* **65**:1410–1421.

Godrijan, J., D. T. Drapeau, and W. M. Balch. 2022. Osmotrophy of dissolved organic carbon by coccolithophores in darkness. *New Phytologist* **233**:781–794.

Gradstein, F. M., J. G. Ogg, M. B. Schmitz, and G. M. Ogg, eds. 2012. *The Geologic Time Scale 2012*. Elsevier, Amsterdam.

Guitián, J., T. Dunkley Jones, I. Hernández-Almeida, T. Löffel, and H. M. Stoll. 2020. Adaptations of coccolithophore size to selective pressures during the Oligocene to Early Miocene high CO_2 world. *Paleoceanography and Paleoclimatology* **35**:e2020PA003918.

Hagino, K., H. Okada, and H. Matsuoka. 2000. Spatial dynamics of coccolithophore assemblages in the equatorial western-central Pacific Ocean. *Marine Micropaleontology* **39**(1–4):53–72.

Hammer, Ø., D. A. Harper, and P.D. Ryan. 2001. PAST: paleontological statistics software package for education and data analysis. *Palaeontologia Electronica* 4(1):4.

Hannisdal, B., J. Henderiks, and L. H. Liow. 2012. Long-term evolutionary and ecological responses of calcifying phytoplankton to changes in atmospheric CO_2. *Global Change Biology* 18:3504–3516.

Hay, W. W., H. P. Mohler, P. H. Roth, R. R. Schmidt, and J. E. Boudreaux. 1967. Calcareous nannoplankton zonation of the Cenozoic of the Gulf Coast and Caribbean-Antillean area, and transoceanic correlation. *Transactions of the Gulf-Coast Association of Geological Societies* 17:428–480.

Henderiks, J. 2008. Coccolithophore size rules—reconstructing ancient cell geometry and cellular calcite quota from fossil coccoliths. *Marine Micropaleontology* 67:143–154.

Henderiks, J., and M. Pagani. 2008. Coccolithophore cell size and the Paleogene decline in atmospheric CO_2. *Earth and Planetary Science Letters* 269:576–584.

Henderiks, J., M. Bartol, N. Pige, B. T. Karatsolis, and B. C. Lougheed. 2020. Shifts in phytoplankton composition and stepwise climate change during the Middle Miocene. *Paleoceanography and Paleoclimatology* 35: e2020PA003915.

Henderiks, J., Sturm, D., Šupraha, L., and Langer, G. 2022. Evolutionary rates in the Haptophyta: exploring molecular and phenotypic diversity. *Journal of Marine Science and Engineering* 10:798.

Holcová, K. 2013. Morphologic variability of the Late Oligocene and the Early Miocene elliptical reticulofenestrids from the Central Paratethys: biostratigraphical, paleoecological and paleogeographical implications. *Acta Palaeontologica Polonica* 58:651–668.

Hutchinson, D. K., H. K. Coxall, D. J. Lunt, M. Steinthorsdottir, A. M. de Boer, M. Baatsen, A. von der Heydt, M. Huber, A. T. Kennedy-Asser, L. Kunzmann, J.-B. Ladant, C. H. Lear, K. Moraweck, P. N. Pearson, E. Piga, M. J. Pound, U. Salzmann, H. D. Scher, W. P. Sijp, K. K. Śliwińska, P. A. Wilson, and Z. Zhang. 2021. The Eocene–Oligocene transition: a review of marine and terrestrial proxy data, models and model–data comparisons. *Climate of the Past* 17:269–315.

Imai, R., M. Farida, T. Sato, and Y. Iryu. 2015. Evidence for eutrophication in the northwestern Pacific and eastern Indian oceans during the Miocene to Pleistocene based on the nannofossil accumulation rate, *Discoaster* abundance, and coccolith size distribution of *Reticulofenestra*. *Marine Micropaleontology* 116:15–27.

Jerkovic, L. 1970. *Noëlaerhabdus nov.* gen. type d'une nouvelle famille de Coccolithophoridés fossiles: Noëlaerhabdaceae du Miocène supérieur de Yougoslavie. Comptes Rendus Hebdomadaires des Séances de l'Académie des Sciences, Paris, série D 270:468–470.

Jones, A. P., and T. Dunkley Jones. 2020. Middle Eocene to Early Oligocene calcareous nannofossils from the Nanggulan Formation, Java, Indonesia. *Journal of Nannoplankton Research* 30:57–79.

Jones, A. P., T. Dunkley Jones, H. Coxall, P. N. Pearson, D. Nala, and M. Hoggett. 2019. Low-latitude calcareous nannofossil response in the Indo-Pacific warm pool across the Eocene–Oligocene transition of Java, Indonesia. *Paleoceanography and Paleoclimatology* 34:1833–1847.

Kamptner, E. 1943. Zur Revision der Coccolithineen-Spezies Pontosphaera huxleyi Lohm. Anzeiger der (Kaiserlichen) Akademie der Wissenschaften, Wien 80:73–49.

Katz, M. E., B. S. Cramer, J. R. Toggweiler, G. Esmay, C. Liu, K. G. Miller, Y. Rosenthal, B. S. Wade, and J. D. Wright. 2011. Impact of Antarctic circumpolar current development on Late Paleogene ocean structure. *Science* 332:1076.

Keller, G. 1983. Paleoclimatic analyses of middle Eocene through Oligocene planktic foraminiferal faunas. *Palaeogeography, Palaeoclimatology, Palaeoecology* 43:73–94.

Kinkel, H., K.-H. Baumann, and M. Cepek. 2000. Coccolithophores in the equatorial Atlantic Ocean: response to seasonal and Late Quaternary surface water variability. *Marine Micropaleontology* 39:87–112.

Langton, S. J., N. M. Rabideaux, C. Borrelli, and M. E. Katz. 2016. Southeastern Atlantic deep-water evolution during the late-middle Eocene to earliest Oligocene (Ocean Drilling Program Site 1263 and Deep Sea Drilling Project Site 366). *Geosphere* 12:1032–1047.

Levin, H. L. 1965. Coccolithophoridae and related microfossils from the Yazoo Formation (Eocene) of Mississippi. *Journal of Paleontology* 39:265–272.

Linnert, C., and Mutterlose, J. 2015. Boreal early Turonian calcareous nannofossils from nearshore settings—implications for Paleoecology. *Palaios* 30:728–742.

Liu, F., M. Gledhill, Q. G. Tan, K. Zhu, Q. Zhang, P. Salaün, A. Tagliabue, Y. Zhang, D. Weiss, E. P. Achterberg, and Y. Korchev. 2022. Phycosphere pH of unicellular nano- and micro-phytoplankton cells and consequences for iron speciation. *ISME Journal* 16:2329–2336.

Lutjeharms, J., and J. Meeuwis. 1987. The extent and variability of south-east Atlantic upwelling. *South African Journal of Marine Science* 5:51–62.

Martini, E. 1971. *Standard Tertiary and Quaternary calcareous nannoplankton zonation.* Pp. 739–785 in Proceedings of the II Planktonic Conference, Roma 1970. Tecnoscienza, Rome.

Martini, E. and S. Ritzkowski. 1968. Was ist das 'Unter-Oligozän'? Eine Analyse der Beyrich'schen und v Koenen'schen Fassung der Stufe mit Hilfe des fossilen Nannoplanktons. *Nachrichten der Akademie der Wissenschaften in Gottingen II. Mathematisch-Physikalische Klasse* 13:231–250.

Marzec, B., J. M. Walker, M. Panagopoulou, Y. Jhons, D. Clare, A. Wheeler, M. P. Shaver, and F. Nudelman. 2019. Three-dimensional architecture and surface functionality of coccolith base plates. *Journal of Structural Biology* 208:127–136.

Matsuoka, H., and H. Okada. 1990. Time-progressive morphometric changes of the genus *Gephyrocapsa* in the Quaternary sequence of the tropical Indian Ocean, Site 709. *Proceedings of the Ocean Drilling Program* 115:255–270.

Milliman, J. D. 1993. Production and accumulation of calcium carbonate in the ocean: budget of a nonsteady state. *Global Biogeochemical Cycles* 7:927–957.

Mitchell, J. G., L. Seuront, M. J. Doubell, D. Losic, N. H. Voelcker, J. Seymour, and R. Lal. 2013. The role of diatom nanostructures in biasing diffusion to improve uptake in a patchy nutrient environment. *PLoS ONE* 8: e59548.

Müller, C. 1970. Nannoplankton aus dem Mittel-Oligozän von Norddeutschland und Belgien. *Neues Jahrbuch für Geologie und Paläontologie, Abhandlungen* 135:82–101.

Müller, M. N., A. N. Antia, and J. LaRoche. 2008. Influence of cell cycle phase on calcification in the coccolithophore *Emiliania huxleyi*. *Limnology and Oceanography* 53:506–512.

Paasche, E. 2001. A review of the coccolithophorid *Emiliania huxleyi* (Prymnesiophyceae), with particular reference to growth, coccolith formation, and calcification-photosynthesis interactions. *Phycologia* 40:503–529.

Pagani, M., M. Huber, Z. Liu, S. M. Bohaty, J. Henderiks, W. Sijp, S. Krishnan, and R. M. DeConto. 2011. The role of carbon dioxide during the onset of Antarctic glaciation. *Science* 334:1261–1264.

Parke, M., and I. Adams. 1960. The motile (*Crystallolithus hyalinus* Gaarder & Markali) and non-motile phases in the life history of *Coccolithus pelagicus* (Wallich) Schiller. *Journal of the Marine Biological Association of the United Kingdom* 39:263–274.

Pascher, A. 1910. Chrysomonaden aus dem Hirschberger Grossteiche: Untersuchungen über die Flora des Hirschberger Grossteiches. I. Teil. *Monographien und Abhandlungen zur Internationale Revue der gesamten Hydrobiologie und Hydrographie* 1:1–66.

Pearson, P. N., G. L. Foster, and B. S. Wade. 2009. Atmospheric carbon dioxide through the Eocene–Oligocene climate transition. *Nature* 461:1110–1113.

Perch-Nielsen, K. 1971. Elektronenmikroskopische Untersuchungen an Coccolithen und verwandten Formen aus dem Eozän von Dänemark. *Det Kongelige Danske Videnskabernes Selskab* 18:1–76.

Perch-Nielsen, K. 1985. Cenozoic calcareous nannofossils. Pp. 329–426 *in* H. M. Bolli, J. B. Saunders, and K. Perch-Nielsen, eds. *Plankton stratigraphy.* Cambridge University Press, Cambridge.

Poulton, A. J., T. R. Adey, W. M. Balch, and P. M. Holligan. 2007. Relating coccolithophore calcification rates to phytoplankton community dynamics: regional differences and implications for carbon export. *Deep-Sea Research, part II (Topical Studies in Oceanography)* 54:538–557.

Poulton, A. J., P. M. Holligan, A. Charalampopoulou, and T. R. Adey. 2017. Coccolithophore ecology in the tropical and subtropical Atlantic Ocean:

new perspectives from the Atlantic meridional transect (AMT) programme. *Progress in Oceanography* **158**:150–170.

Proto Decima, F., F. Medizza, F. and L. Todesco. 1978. Southeastern Atlantic Leg 40 calcareous nannofossils. Pp. 571–634 *in* H. M. Bolli, W. B. F. Ryan, J. B. Foresman, W. E. Hottman, H. Kagami, J. F. Longoria, B. K. McKnight, *et al. Initial Reports of the Deep Sea Drilling Project*, Vol. **40**. Texas A&M University, Ocean Drilling Program, College Station, Tex.

Pusz, A. E., R. C. Thunell, and K. G. Miller. 2011. Deep water temperature, carbonate ion, and ice volume changes across the Eocene–Oligocene climate transition. *Paleoceanography* **26**(2). https://doi.org/10.1029/2010PA001950.

Rae, J. W., Zhang, Y. G., Liu, X., Foster, G. L., Stoll, H. M., and Whiteford, R. D. 2021. Atmospheric CO_2 over the past 66 million years from marine archives. *Annual Review of Earth and Planetary Sciences* **49**:609–641.

Rokitta, S. D., L.J. de Nooijer, S. Trimborn, C. de Vargas, B. Rost, and U. John. 2011. Transcriptome analyses reveal differential gene expression patterns between the life-cycle stages of *Emiliania huxleyi* (Haptophyta) and reflect specialization to different ecological niches. *Journal of Phycology* **47**:829–838.

Roth, P. H. 1970. Oligocene calcareous nannoplankton biostratigraphy. *Eclogae Geologicae Helvetiae* **63**:799–881.

Sarmiento, J. L., N. Gruber, M. Brzezinski, and J. Dunne. 2004. High-latitude controls of thermocline nutrients and low latitude biological productivity. *Nature* **427**:56–60.

Schindelin, J., I. Arganda-Carreras, E. Frise, V. Kaynig, M. Longair, T. Pietzsch, A. Cardona. 2012. Fiji: an open-source platform for biological-image analysis. *Nature Methods* **9**:676–682.

Segev, E., T. P. Wyche, K. H. Kim, J. Petersen, C. Ellebrandt, H. Vlamakis, N. Barteneva, J. N. Paulson, L. Chai, J. Clardy, and R. Kolter. 2016. Dynamic metabolic exchange governs a marine algal-bacterial interaction. *eLife* **5**:e17473.

Seymour, J. R., S. A. Amin, J. B. Raina, and R. Stocker. 2017. Zooming in on the phycosphere: the ecological interface for phytoplankton-bacteria relationships. *Nature Microbiology* **2**:17065.

Selosse, M. A., M. Charpin, and F. Not. 2017. Mixotrophy everywhere on land and in water: the grand écart hypothesis. *Ecology Letters* **20**:246–263.

Shackleton, N. J. 1975. Paleotemperature history of the Cenozoic and the initiation of Antarctic glaciation: oxygen and carbon isotope analyses in DSDP Sites 277, 279, and 281. *Initial Reports of the Deep Sea Drilling Project* **29**:743–755.

Sheward, R. M., A. J. Poulton, S. J. Gibbs, C. J. Daniels and P. R. Bown. 2017. Physiology regulates the relationship between coccosphere geometry and growth phase in coccolithophores. *Biogeosciences* **14**:1493–1509.

Smriga, S., V. I. Fernandez, J. G. Mitchell, and R. Stocker. 2016. Chemotaxis toward phytoplankton drives organic matter partitioning among marine bacteria. *Proceedings of the National Academy of Sciences USA* **113**:1576–1581.

Stradner, H., and A. R. Edwards. 1968. Electron microscopic studies on upper Eocene coccoliths from the Oamaru diatomite, New Zealand. *Jahrbuch der Geologischen Bundesanstalt* **13**:1–66.

Suchéras-Marx, B., E. Mattioli, B. Pittet, G. Escarguel, and G. Suan. 2010. Astronomically-paced coccolith size variations during the early Pliensbachian (Early Jurassic). *Palaeogeography, Palaeoclimatology, Palaeoecology* **295**:281–292.

Suchéras-Marx, B., E. Mattioli, P. Allemand, F. Giraud, B. Pittet, J. Plancq, and G. Escarguel. 2019. The colonization of the oceans by calcifying pelagic algae. *Biogeosciences* **16**:2501–2510.

Taylor, A. R., C. Brownlee, and G. Wheeler. 2017. Coccolithophore cell biology: chalking up progress. *Annual Review of Marine Science* **9**:283–310.

Theodoridis, S. 1984. Calcareous nannofossil biostratigraphy of the Miocene and revision of the helicoliths and discoasters. *Utrecht Micropaleontological Bulletin* **32**:1–271.

Toumarkine, M. 1978. Planktonic foraminiferal biostratigraphy of the Paleogene of Sites 360 to 364 and the Neogene of Sites 362A, 363, and 364 Leg 40. Pp. 571–634 *in* H. M. Bolli, W. B. F. Ryan, J. B. Foresman, W. E. Hottman, H. Kagami, J. F. Longoria, B. K. McKnight, *et al. Initial Reports of the Deep Sea Drilling Project*, Vol. **40**. Texas A&M University, Ocean Drilling Program, College Station, Tex.

Villa, G., C. Fioroni, D. Persico, A. P. Roberts, and F. Florindo. 2014. Middle Eocene to Late Oligocene Antarctic glaciation/deglaciation and Southern Ocean productivity. *Paleoceanography* **29**:2013PA002518.

Villa, G., F. Florindo, D. Persico, P. Lurcock, A. P. de Martini, L. Jovane, and C. Fioroni. 2021. Integrated calcareous nannofossil and magnetostratigraphic record of ODP Site 709: Middle Eocene to late Oligocene paleoclimate and paleoceanography of the Equatorial Indian Ocean. *Marine Micropaleontology* **169**:102051.

Wei, W., and S. W. Wise. 1990. Biogeographic gradients of middle Eocene–Oligocene calcareous nannoplankton in the South Atlantic Ocean. *Palaeogeography, Palaeoclimatology, Palaeoecology* **79**:29–61.

Wise, S. 1983. Mesozoic and Cenozoic calcareous nannofossils recovered by DSDP leg 71 in the Falkland Plateau region, SW Atlantic Ocean. *Initial Reports of the Deep Sea Drilling Project* **71**:481–551.

Young, J. R. 1987. Possible functional interpretations of coccolith morphology. *Abhandlungen der Geologischen Bundesanstalt.-A* **39**:305–313.

Young, J. R. 1989. Observations on heterococcolith rim structure and its relationship to developmental processes. Pp. 1–20 *in* J. Crux and S. E. van Heck, eds. *Nannofossils and their applications: Proceedings of the Second International Nannoplankton Association Symposium, London.* Ellis Horwood, Chichester, U.K.

Young, J. R. 1990. Size variation of Neogene *Reticulofenestra* coccoliths from Indian Ocean DSDP cores. *Journal of Micropalaeontology* **9**:71–85.

Young, J. R., and P. R. Bown. 1997. Cenozoic calcareous nannoplankton classification. *Journal of Nannoplankton Research* **19**:36–47.

Young, J. R., H. Andruleit, and I. Probert. 2009. Coccolith function and morphogenesis: insights from appendage-bearing coccolithophores of the family Syracosphaeraceae (Haptophyta) (1). *Journal of Phycology* **45**:213–226.

Zachos, J. C., T. M. Quinn, and K. A. Salamy. 1996. High-resolution (10^4 years) deep-sea foraminiferal stable isotope records of the Eocene–Oligocene climate transition. *Paleoceanography* **11**:251–266.

Zhang, Y. G., M. Pagani, M., Z. Liu, S. M. Bohaty, and R. DeConto. 2013. A 40-million-year history of atmospheric CO_2. *Philosophical Transactions of the Royal Society of London A* **371**:20130096.